

# Part Dimensional Error and Its Propagation Modeling in Multi-Operational Machining Processes

Qiang Huang  
Jianjun Shi\*

Department of Industrial and Operations  
Engineering,  
The University of Michigan,  
Ann Arbor, MI 48109

Jingxia Yuan

Department of Mechanical Engineering,  
The University of Michigan,  
Ann Arbor, MI 48109

*In a multi-operational machining process (MMP), the final product variation is an accumulation or stack-up of variation from all machining operations. Modeling and control of the variation propagation is essential to improve product dimensional quality. This paper presents a state space model and its modeling strategies to describe the variation stack-up in MMPs. The physical relationship is explored between part variation and operational errors. By using the homogeneous transformation approach, kinematic modeling of setup and machining operations are developed. A case study with real machined parts is presented in the model validation. [DOI: 10.1115/1.1532007]*

## 1 Introduction

A machining process is typically a discrete and multi-operational process with multivariate quality characteristics. Variation reduction and quality improvement is a very important and challenging topic, especially for complicated parts with tight tolerances, multiple operations and frequent changes of datums. Part variations can be attributed to process sequence, datums, fixtures, and machine tools. In addition, variations usually propagate from upstream to downstream operations. Since modeling variation stack-up facilitates design optimization, process control, and root cause diagnosis, it has been studied in many fields.

In tolerance design, a variety of tolerance stack-up models have been studied, including the worst case (WC) model, the root sum square (RSS) model [1], the inflated RSS model [2], and the estimated mean shifted model [3]. In these models, the stack-up function  $Y = f(x_1, x_2, \dots, x_n)$  is frequently applied to describe the relationship between the assembly dimension  $Y$  and component feature dimensions  $x_1, x_2, \dots, x_n$ . However, it is hard to make tenable assumptions on the distributions of  $x_i$ 's, because they depend on specific design and operation details of a process. Ding et al. [4] proposed so-called process-oriented tolerance synthesis approach by modeling product and process variables together. Instead of the stack-up function, a state space model is employed and fixture tolerances for each station are allocated simultaneously with minimum cost.

The studies on state space modeling of assembly processes can be traced back to Jin and Shi [5], where the initiatives are for the purpose of process monitoring and diagnosis. Three different errors caused by fixtures were studied and the state space form was applied to describe the error propagation. This study was extended by considering the situation that more than two sheet metal parts are welded together at one station [6]. Mantripragada and Whitney [7] proposed a state transition model in which the fixture is assumed to be perfect and only part fabrication imperfection is considered. Lawless et al. [8,9] used an autoregressive model to analyze the variation transmission problem. Their data-driven approach primarily depends on the historical data. In addition, the same product characteristics need to be tracked at each station, which limits the applicability of that approach.

Modeling the physics of variation propagation is surprisingly a

less explored area for MMPs. The main reason could be due to the part and process complexities. Most of the studies focused on single machine station problems, such as the robust fixture design to minimize the workpiece positional errors [10], investigation of the impact of fixture locator tolerance scheme on datum establishment errors [11], or machine tool error compensation study [12].

The purpose of this paper is to develop a state space model to describe part error propagation in MMPs. The remainder of the paper includes six sections. Section 2 briefly introduces machining processes and defines error sources. Section 3 presents a quality-oriented part model to facilitate part deviation representation. Kinematic modeling of machining and setup operations is presented in Section 4. Section 5 applies the state space form to recursively describe part error propagation. In Section 6, the developed model is validated by cutting experiments under normal and faulty conditions. A summary is given in Section 7.

## 2 Machining Processes and Error Accumulation

In an MMP, not only the metal cutting (i.e., the machining operation), but also the setup operation (part locating and orientation) affects part quality. The induced part error will propagate through the process, especially when operations correlate with each other. The main correlation is caused by the datum effect, i.e., if previous machined surfaces are used as the datum in the current operation, the datum imperfection often affects the accuracy of currently machined surfaces.

Figure 1 shows the error propagation in a machining process with  $N$  operations. Operation  $k$  ( $k=1, \dots, N$ ) is defined as the  $k$ th setup and the cutting operation based on that setup. In general, the number of machine stations can be smaller than the number of operations, because there may have more than one setup operation within the same station. The main error sources at operation  $k$  are classified as: 1) fixture error  $\mathbf{e}_k^f$  (geometric inaccuracy of locating elements), 2) datum errors  $\mathbf{e}_k^d$  due to the imperfection of datum surfaces, 3) machine tool errors  $\mathbf{e}_k^m$  (volumetric errors [12]), and 4) noise  $\mathbf{w}(k)$  due to process natural variations. Assume that  $\mathbf{e}_k^f$ ,  $\mathbf{e}_k^d$ ,  $\mathbf{e}_k^m$  and  $\mathbf{w}(k)$  are independent.

Setup error  $\mathbf{e}_k^s$  is the error jointly caused by  $\mathbf{e}_k^f$  and  $\mathbf{e}_k^d$  in the  $k$ th setup operation. Machine tool error  $\mathbf{e}_k^m$ , often referred to as the tool path error, is the error generated by the  $k$ th cutting operation.

## 3 Part Model, Part Deviation, and Observation

Intermediate and final part deviation is of direct interest in modeling part dimensional error and error propagation. Part models

\*Author to whom all correspondence should be addressed. J. Shi, Tel:734-763-5321, Fax: 734-764-3451. Email: shihang@umich.edu

Contributed by the Manufacturing Engineering Division for publication in the Journal of Manufacturing Science and Engineering. Manuscript received October 2001; Revised July 2002. Associate Editor: E. C. De Meter.

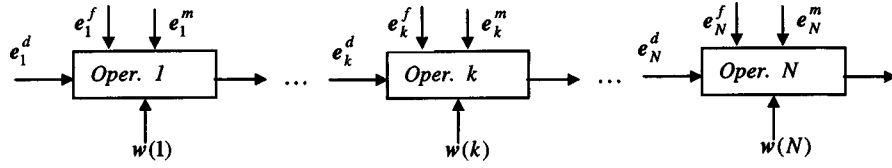


Fig. 1 Error propagation in MMPs

need only to describe features relevant to part deviation. Therefore, a revised vectorial surface model is applied to represent the part. More details about vectorial surface modeling can be found in [13].

**Part Model.** Suppose a part has  $n$  surfaces related to the error propagation. Those  $n$  surfaces include surfaces to be machined, design datums, machining datums and measurement datums. In a coordinate system, the  $i$ th surface  $\mathbf{X}_i$  can be described by its surface orientation  $\mathbf{n}_i = [n_{ix}, n_{iy}, n_{iz}]^T$ , location  $\mathbf{p}_i = [p_{ix}, p_{iy}, p_{iz}]^T$ , and size  $\mathbf{D}_i = [d_{i1}, d_{i2}, \dots, d_{im}]^T$ . By stacking up  $\mathbf{n}_i$ ,  $\mathbf{p}_i$ , and  $\mathbf{D}_i$ ,  $\mathbf{X}_i$  is represented as a vector with dimension  $(6+m)$ , that is,

$$\mathbf{X}_i = [\mathbf{n}_i^T, \mathbf{p}_i^T, \mathbf{D}_i^T]^T_{(6+m) \times 1} \quad (1)$$

where  $m$  is the number of size parameters in  $\mathbf{D}_i$ . Size parameter here has broader meaning than that for the dimension of size given by GD&T [14]. It can be the diameter, flatness, or parallelism.

With the representation for individual part surface, the part is modeled as a vector by stacking up all surface vectors, that is,

$$\mathbf{X} = [\mathbf{X}_1^T, \mathbf{X}_2^T, \dots, \mathbf{X}_n^T]^T \quad (2)$$

**Part Deviation.** Due to operational errors and natural process variation, machined part features might deviate from their ideal counterparts. The feature deviation can be derived from Eq. (1), that is, the deviation of surface  $\mathbf{X}_i$  from the ideal surface  $\mathbf{X}_i^o$  (in this paper, variable with superscript “ $o$ ” denotes the nominal value of that variable) is

$$\Delta \mathbf{X}_i = [\Delta \mathbf{n}_i^T, \Delta \mathbf{p}_i^T, \Delta \mathbf{D}_i^T]^T \quad (3)$$

where  $\Delta \mathbf{n}_i = [\Delta n_{ix}, \Delta n_{iy}, \Delta n_{iz}]^T$ ,  $\Delta \mathbf{p}_i = [\Delta p_{ix}, \Delta p_{iy}, \Delta p_{iz}]^T$  and  $\Delta \mathbf{D}_i = [\Delta d_{i1}, \Delta d_{i2}, \dots, \Delta d_{im}]^T$ . An example for a cylinder surface is illustrated in Fig. 2.

Let  $\mathbf{x}$  denote part deviation  $\Delta \mathbf{X}$ . By Eqs. (2) and (3),  $\mathbf{x}$  is

$$\mathbf{x} = [\Delta \mathbf{X}_1^T, \Delta \mathbf{X}_2^T, \dots, \Delta \mathbf{X}_n^T]^T \quad (4)$$

Use  $\mathbf{x}(k)$  to index the intermediate part deviation after operation  $k$ .

**Observation of Part Deviation.** Suppose  $p$  part characteristics  $\mathbf{Y} = [Y_1, \dots, Y_p]^T$  are measured. The deviation of  $\mathbf{Y}$  from design specifications, i.e.,  $\Delta \mathbf{Y} = [\Delta Y_1, \dots, \Delta Y_p]^T$ , represents the ob-

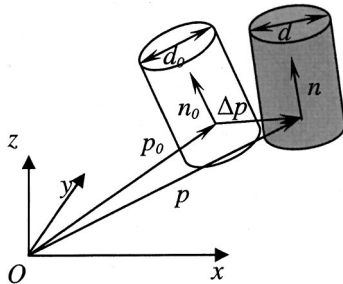


Fig. 2 Cylinder surface and surface deviation representation

servations of part deviation  $\mathbf{x}$ . Similarly, denote  $\Delta \mathbf{Y}$  as  $\mathbf{y}$  and index intermediate observation as  $\mathbf{y}(k)$ , if the measurement is taken at operation  $k$ .

$Y_i (1 \leq i \leq p)$  is a function of  $\mathbf{X}$ , i.e.,  $Y_i = G_i(\mathbf{X})$ . For example,  $Y_i$  might be the distance between two planes. If part deviation  $\mathbf{x}$  is small, Taylor series expansion can be used to approximate the function  $G_i$  by a linear component  $\mathbf{C}_i \mathbf{x}$  plus a noise term  $\nu_i$ , that is,

$$\Delta Y_i = \mathbf{C}_i \mathbf{x} + \nu_i \quad (5)$$

where  $\mathbf{C}_i = [dG_i/d\mathbf{X}^T]_{1 \times n(6+m)}$  and  $\nu_i$  includes the high order terms from Taylor series expansion and measurement errors. By Eq. (5),  $\mathbf{y}$  is expressed as

$$\mathbf{y} = \mathbf{C} \mathbf{x} + \boldsymbol{\nu} \quad (6)$$

$$\mathbf{C} = \begin{bmatrix} \mathbf{C}_1 \\ \vdots \\ \mathbf{C}_p \end{bmatrix}_{p \times n(6+m)} \quad (7)$$

where  $\mathbf{C}$  is defined as the sensitivity matrix, transforming the part deviation  $\mathbf{x}$  to observed deviation  $\mathbf{y}$ .  $\boldsymbol{\nu} = [\nu_1, \nu_2, \dots, \nu_p]^T$  is the noise term.

## 4 Setup and Machining Operation

Part deviation is mainly caused by setup and machining operations. During each operation, the part is fixed in a fixture and then cut in the machine tool. Three coordinate systems are introduced as references to describe the part deviation and operational errors. Naturally the homogeneous transformation approach is applied to depict part transformation among coordinates and to model how the operational errors affect the part quality during the transformation. This is the main focus of this section, that is, kinematic modeling of machining and setup operations.

### 4.1 Coordinate Systems.

- M-Coordinate: the machine tool coordinate  $(x_M, y_M, z_M)$ , in which the fixture is located and oriented on the machine table.
- F-Coordinate: the fixture coordinate  $(x_F, y_F, z_F)$ , built in the fixture in which the part is located and oriented.
- P-Coordinate: the part coordinate  $(x, y, z)$ , in which the part surfaces are represented. The subscription “P” is omitted for simplicity (Fig. 3).

Let  $\mathbf{X}$ ,  $\mathbf{X}_F$  and  $\mathbf{X}_M$  be the part represented in the P-Coordinate, F-Coordinate and M-Coordinate respectively. The homogeneous transformation is used to model the part transformation among coordinates through rotation and translation transformations. For example, before machining, the part needs to be fixed into a fixture on the machine tool table (This operation is called setup and will be further discussed in Section 4.2). The procedure is modeled as transforming the part from P-Coordinate to F-Coordinate and then from F-Coordinate to M-Coordinate. The mathematical expression is given by Eq. (8),

$$\begin{bmatrix} \mathbf{X}_F \\ \mathbf{1} \end{bmatrix} = \begin{bmatrix} {}^F R_P & {}^F \mathbf{T}_P \\ \mathbf{0} & \mathbf{1} \end{bmatrix} \begin{bmatrix} \mathbf{X} \\ \mathbf{1} \end{bmatrix} \quad \text{and} \quad \begin{bmatrix} \mathbf{X}_M \\ \mathbf{1} \end{bmatrix} = \begin{bmatrix} {}^M R_F & {}^M \mathbf{T}_F \\ \mathbf{0} & \mathbf{1} \end{bmatrix} \begin{bmatrix} \mathbf{X}_F \\ \mathbf{1} \end{bmatrix} \quad (8)$$

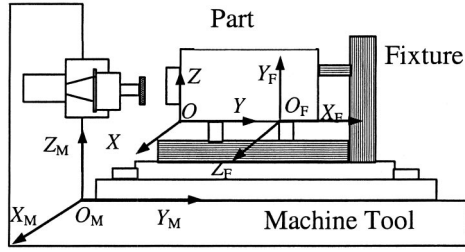


Fig. 3 Coordinate systems

where “**1**” is a vector with all ones and “**0**” is zero matrix. Translation vector  ${}^M\mathbf{T}_F$  is defined as

$${}^M\mathbf{T}_F = \left[ \underbrace{O_F, O_F, \dots, O_F}_n \right]^T \text{ with } O_F = \left[ \underbrace{0, 0, 0, x_F, y_F, z_F}_m, \underbrace{0, \dots, 0}_m \right] \quad (9a)$$

where  $(x_F, y_F, z_F)$  is the coordinate of the origin of the F-Coordinate in the M-Coordinate. Similarly, we have

$${}^F\mathbf{T}_P = \left[ \underbrace{O, O, \dots, O}_n \right]^T \text{ with } O = \left[ \underbrace{0, 0, 0, x, y, z}_m, \underbrace{0, \dots, 0}_m \right] \quad (9b)$$

where  $(x, y, z)$  is the coordinate of the origin of the P-Coordinate in the F-Coordinate.

Rotation matrix  ${}^M R_F$  is defined as

$${}^M R_F = \text{diag}(\underbrace{R_F, \dots, R_F}_n) \text{ with } R_F = \text{diag}({}^M R_{O_F}, {}^M R_{O_F}, I_{m \times m}) \quad (10)$$

where  ${}^M R_{O_F} = [{}^M \mathbf{u}_F, {}^M \mathbf{v}_F, {}^M \mathbf{w}_F]_{3 \times 3}$  and  ${}^M \mathbf{u}_F, {}^M \mathbf{v}_F$  and  ${}^M \mathbf{w}_F$  denote three unit vectors pointing along the axes of the F-Coordinate in the M-Coordinate.  $I_{m \times m}$  is the identity matrix.

${}^F R_P$  is defined as

$${}^F R_P = \text{diag}(\underbrace{R_P, \dots, R_P}_n) \text{ with } R_P = \text{diag}({}^F R_{O_P}, {}^F R_{O_P}, I_{m \times m}) \quad (11)$$

where  ${}^F R_{O_P} = [{}^F \mathbf{u}_P, {}^F \mathbf{v}_P, {}^F \mathbf{w}_P]_{3 \times 3}$  and  ${}^F \mathbf{u}_P, {}^F \mathbf{v}_P$  and  ${}^F \mathbf{w}_P$  denote three unit vectors pointing along the axes of the P-Coordinate in the F-Coordinate.

**4.2 Setup Operation.** Setup consists of two steps, that is, position the workpiece on a fixture, and then locate the fixture on a machine tool table. Equation (8) models the two-step procedure. An alternative is to model setup as a direct transformation from the P-Coordinate to the M-Coordinate. For the  $k$ th setup, the incoming workpiece  $\mathbf{X}(k-1)$  is transformed to  $\mathbf{X}_M(k-1)$  in the M-Coordinate through a rotation transformation  ${}^M R_P(k)$  and a translation transformation  ${}^M \mathbf{T}_P(k)$ , that is,

$$\mathbf{X}_M(k-1) = {}^M R_P(k) \mathbf{X}(k-1) + {}^M \mathbf{T}_P(k) \quad (12a)$$

where  ${}^M R_P(k)$  and  ${}^M \mathbf{T}_P(k)$  can be obtained from Eq. (8) as

$${}^M R_P(k) = {}^M R_F(k) {}^F R_P(k) \text{ and } {}^M \mathbf{T}_P(k) = {}^M R_F(k) {}^F \mathbf{T}_P(k) + {}^M \mathbf{T}_F(k) \quad (12b)$$

where  ${}^F R_P(k), {}^F \mathbf{T}_P(k), {}^M R_F(k)$  and  ${}^M \mathbf{T}_F(k)$  represent  ${}^F R_P, {}^F \mathbf{T}_P, {}^M R_F$  and  ${}^M \mathbf{T}_F$  at operation  $k$ . The following relationship still holds:

$${}^P R_M(k) = ({}^M R_P(k))^{-1} = ({}^M R_F(k) {}^F R_P(k))^{-1} = {}^P R_F(k) {}^F R_M(k) \quad (12c)$$

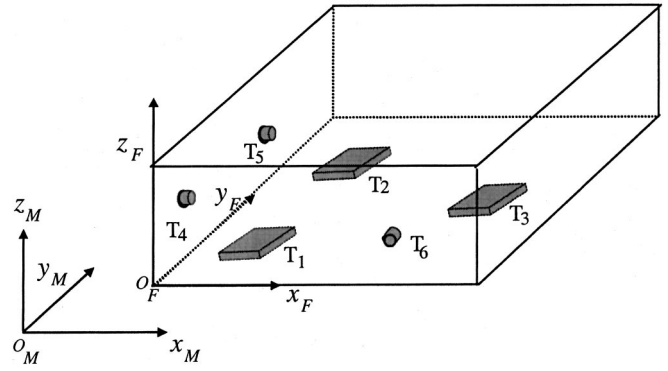


Fig. 4 Fixture with 3-2-1 locating scheme

The fact is that in the two-step procedure of setup, the fixture affects the coordinate transformation between the F-Coordinate and M-Coordinate, while the datum affects the coordinate transformation between the P-Coordinate and F-Coordinate. The part deviation might be generated due to improperly positioning the part in the M-Coordinate. To assess the impact of fixture errors and datum errors on part quality, we need to model fixture and datum and to study how those two types of errors affect setup.

In order to illustrate fixture deviations, the study uses the popular 3-2-1 locating scheme (Fig. 4). The same methodology can be followed for other locating schemes.

Six fixture tooling elements  $T_i$ 's ( $i = 1, 2, \dots, 6$ ) are sufficient to restrict the six degrees of freedom of the part. In the contact area of tooling element  $T_i$  with the datum surface, the position of an arbitrary point is used to represent the position of  $T_i$  in the M-Coordinate, denoted as  $(T_{ix_M}, T_{iy_M}, T_{iz_M})$ . Since  $T_{1z_M}, T_{2z_M}, T_{3z_M}, T_{4x_M}, T_{5x_M}$  and  $T_{6y_M}$  are sufficient to determine the F-Coordinate, a vector  $\mathbf{T}_E$  is defined to represent the fixture:

$$\mathbf{T}_E = [T_{1z_M}, T_{2z_M}, T_{3z_M}, T_{4x_M}, T_{5x_M}, T_{6y_M}]^T \quad (13)$$

The fixture deviation is caused by the deviations of tooling elements, which is defined as

$$\Delta \mathbf{T}_E = [\Delta T_{1z_M}, \Delta T_{2z_M}, \Delta T_{3z_M}, \Delta T_{4x_M}, \Delta T_{5x_M}, \Delta T_{6y_M}]^T \quad (14)$$

At operation  $k$ , only fixture  $\mathbf{T}_E$  (indexed by  $\mathbf{T}_E(k)$ ) affects  ${}^M R_F$  and  ${}^M \mathbf{T}_F$ . Therefore, transformation deviation of  ${}^M R_F(k)$  and  ${}^M \mathbf{T}_F(k)$  is caused by fixture deviation  $\Delta \mathbf{T}_E(k)$ . Under a small deviation assumption, the transformation deviation is approximated by the first order Taylor series expansion, that is,

$$\Delta {}^M R_F(k) = \left[ \frac{d({}^M R_F(k))_{ij}}{d\mathbf{T}_E(k)^T} \Delta \mathbf{T}_E(k) \right]_{n(6+m) \times n(6+m)} \quad (15a)$$

$$\Delta {}^M \mathbf{T}_F(k) = \left[ \frac{d({}^M \mathbf{T}_F(k))_i}{d\mathbf{T}_E(k)^T} \Delta \mathbf{T}_E(k) \right]_{n(6+m) \times 1} \quad (15b)$$

where  $({}^M R_F(k))_{ij}$  denotes the  $i$ th row and the  $j$ th column of  ${}^M R_F(k)$ , and  $({}^M \mathbf{T}_F(k))_i$  denotes the  $i$ th row of  ${}^M \mathbf{T}_F(k)$ .

As a result, the actual transformation from F-Coordinate to M-Coordinate is represented by the summation of a nominal transformation and the deviation caused by fixture errors, that is,

$${}^M R_F(k) = {}^M R_F^o(k) + \Delta {}^M R_F(k) \quad (16a)$$

$${}^M \mathbf{T}_F(k) = {}^M \mathbf{T}_F^o(k) + \Delta {}^M \mathbf{T}_F(k) \quad (16b)$$

${}^F R_P$  and  ${}^F \mathbf{T}_P$  are affected by datum. Before introducing datum deviation, we introduce a datum selection matrix  $D(k)$  as

$$D(k) = \text{diag}((J_1)_{(6+m) \times (6+m)}, \dots, (J_n)_{(6+m) \times (6+m)}) \quad (17)$$

where  $J_i$  is a diagonal matrix only with “1” and/or “0” as data entries and  $m$  is the dimension of size parameters in  $\mathbf{X}(k)$ .

From the incoming workpiece  $\mathbf{X}(k-1)$ ,  $D(k)$  selects part surfaces used for datum at operation  $k$ . To select surface  $\mathbf{X}_i$  as the primary datum,  $J_i$  is constructed as  $\text{diag}(1,1,1,0 \dots 0)$ , which specifies the orientation of the primary datum. For the secondary or the tertiary datum,  $J_i$  is constructed by choosing the position component of a surface. Denote the datum as  $\mathbf{D}_E(k)$  with

$$\mathbf{D}_E(k) = D(k)\mathbf{X}(k-1) \quad (18)$$

The datum deviation is represented as the deviation of those selected part surfaces, that is,

$$\Delta \mathbf{D}_E(k) = D(k)\mathbf{x}(k-1) \quad (19)$$

If the datum  $\mathbf{D}_E(k)$  firmly contacts with tooling elements of fixture  $\mathbf{T}_E(k)$ , the transformation matrices  ${}^F R_p(k)$  and  ${}^F \mathbf{T}_p(k)$  are determined, which are functions of  $\mathbf{D}_E(k)$ . Follow Eq. (15), the deviation of  ${}^F R_p(k)$  and  ${}^F \mathbf{T}_p(k)$  caused by  $\Delta \mathbf{D}_E(k)$  can be expressed as

$$\Delta {}^F R_p(k) = \left[ \frac{d({}^F R_p(k))_{ij}}{d\mathbf{D}_E(k)^T} \Delta \mathbf{D}_E(k) \right]_{n(6+m) \times n(6+m)} \quad (20a)$$

$$\Delta {}^F \mathbf{T}_p(k) = \left[ \frac{d({}^F \mathbf{T}_p(k))_i}{d\mathbf{D}_E(k)^T} \Delta \mathbf{D}_E(k) \right]_{n(6+m) \times 1} \quad (20b)$$

Similarly, the actual transformation from P-Coordinate to F-Coordinate is represented by the summation of a nominal transformation and the deviation caused by datum errors, that is,

$${}^F R_p(k) = {}^F R_p^o(k) + \Delta {}^F R_p(k) \quad (21a)$$

$${}^F \mathbf{T}_p(k) = {}^F \mathbf{T}_p^o(k) + \Delta {}^F \mathbf{T}_p(k) \quad (21b)$$

The joint effect of fixture errors and datum errors on setup can now be described by plugging Eqs. (16) and (21) into Eq. (12). Neglecting high order terms, we have

$$\begin{aligned} {}^M R_p(k) &= {}^M R_F^o(k) {}^F R_p^o(k) + [{}^M R_F^o(k) \Delta {}^F R_p(k) \\ &\quad + \Delta {}^M R_F(k) {}^F R_p^o(k)] \end{aligned} \quad (22a)$$

$$\begin{aligned} {}^M \mathbf{T}_p(k) &= [{}^M R_F^o(k) {}^F \mathbf{T}_p^o(k) + {}^M \mathbf{T}_F^o(k)] + [\Delta {}^M R_F(k) {}^F \mathbf{T}_p^o(k) \\ &\quad + {}^M R_F^o(k) \Delta {}^F \mathbf{T}_p(k) + \Delta {}^M \mathbf{T}_F(k)] \end{aligned} \quad (22b)$$

$$\Delta {}^M R_p(k) = {}^M R_F^o(k) \Delta {}^F R_p(k) + \Delta {}^M R_F(k) {}^F R_p^o(k) \quad (22c)$$

$$\Delta {}^M \mathbf{T}_p(k) = \Delta {}^M R_F(k) {}^F \mathbf{T}_p^o(k) + {}^M R_F^o(k) \Delta {}^F \mathbf{T}_p(k) + \Delta {}^M \mathbf{T}_F(k) \quad (22d)$$

Up to now, fixture error  $\mathbf{e}_k^f$  and datum error  $\mathbf{e}_k^d$  can be explicitly expressed by Eqs. (14) and (19), i.e.,  $\mathbf{e}_k^d = \Delta \mathbf{T}_E(k)$  and  $\mathbf{e}_k^f = \Delta \mathbf{D}_E(k)$ . Setup error  $e_k^s$  is expressed by Eqs. (22c) and (22d).

**4.3 Machining Operation.** After the setup operation transforms the workpiece  $\mathbf{X}(k-1)$  to  $\mathbf{X}_M(k-1)$ , the  $k$ th machining

operation generates new part  $\mathbf{X}_M(k)$ , which can be divided into the machined surfaces  $B(k)\mathbf{X}_M^u(k)$  and the uncut surfaces  $A(k)\mathbf{X}_M(k-1)$ , that is,

$$\mathbf{X}_M(k) = A(k)\mathbf{X}_M(k-1) + B(k)\mathbf{X}_M^u(k) \quad (23)$$

where  $B(k)$  labels all surfaces to be machined at operation  $k$ , defined as

$$B(k) = \text{diag}((I_1)_{(6+m) \times (6+m)}, \dots, (I_n)_{(6+m) \times (6+m)}) \quad (24a)$$

and  $(I_i)_{(6+m) \times (6+m)} (1 \leq i \leq n)$  is an indicator matrix for  $\mathbf{X}_i$ , defined as

$$I_i = \begin{cases} I_{(6+m) \times (6+m)}, & \text{surface } \mathbf{X}_i \text{ is machined at operation } k \\ \mathbf{0}, & \text{Otherwise} \end{cases} \quad (24b)$$

where  $I_{(6+m) \times (6+m)}$  is the identity matrix and “0” is the zero matrix.

$B(k)$  is a representation of the process sequence, while  $A(k)$  is defined as  $A(k) = I - B(k)$ , labeling uncut surfaces at operation  $k$ .

By transforming  $\mathbf{X}_M(k)$  back to the P-Coordinate, the part deviation is expressed as

$$\mathbf{x}(k) = A(k)\mathbf{x}(k-1) + B(k)\mathbf{x}^u(k) + \mathbf{w}(k) \quad (25)$$

where noise term  $\mathbf{w}(k)$  includes neglected high order error terms and natural process variation.

In the M-Coordinate, only machine tool error  $e_k^m$  causes deviations of newly machined part surfaces  $B(k)\mathbf{X}_M^u(k)$ . Depending on the problem domains,  $e_k^m$  can be as complicated as the volumetric error model [12], or a simplified kinematic machine tool model [15]. Since the purpose of this research is to model process variation propagation, distinguishing each machine tool error component is unnecessary. In this study, each surface deviation in  $B(k)\mathbf{x}_M^u$  is treated as a projection of machine tool error  $e_k^m$  on that surface. The projections vary with surface orientations. Thus the projected machine tool error  $P(e_k^m)_i$  onto the  $i$ th surface  $(B(k)\mathbf{x}_M^u(k))_i$  is represented as

$$P(e_k^m)_i = (B(k)\mathbf{x}_M^u(k))_i \quad (26)$$

Corresponding to the size parameters of surfaces, the size component of  $e_k^m$  represents tool size related errors. With this, the total part deviations induced by  $e_k^m$  are expressed as

$$B(k)\mathbf{x}_M^u(k) = B(k)[X_M^u(k) - X_M^o(k)] \quad (27)$$

Based on the knowledge of machine tool capability, we assume the deviation  $B(k)\mathbf{x}_M^u(k)$  follows multivariate normal distribution.

## 5 Deviation Propagation Model

With the preparation work in Section 4, we are ready to describe how the datum errors, fixture errors, and machine tool errors cause part deviation for each operation (Fig. 5). The result is

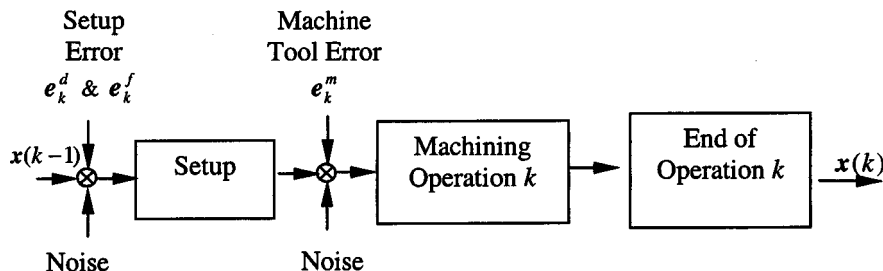


Fig. 5 Error propagation

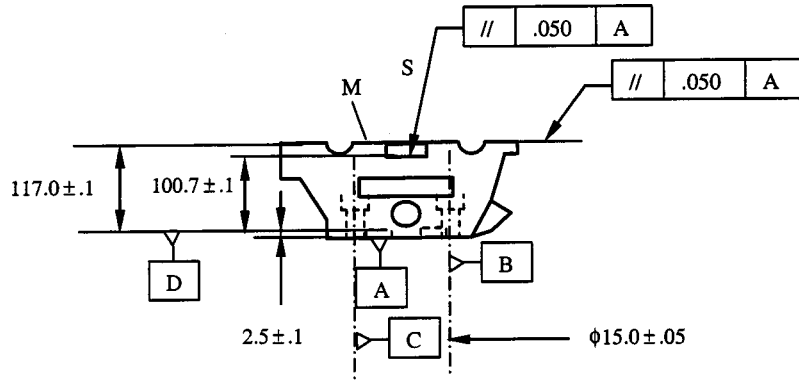


Fig. 6 Design specifications of cylinder head

Table 1 Description of Characteristics

Characteristics	Specifications(mm)	Operation
(1) Distance btw cover face M and datum surface D	117.0±0.1	1st
(2) Distance btw joint face A and datum surface D	2.50±0.1	
(3) Parallelism btw M and A	0.050	2nd
(4) Diameter of hole B	15.00±0.05	
(5) Distance btw slot S and D	100.7±0.1	3rd
(6) Parallelism btw A and S	0.050	

given by the following proposition (See the derivation in the Appendix).

**Proposition 1** The error propagation model in a MMP is proposed as

$$\mathbf{x}(k) = A(k)\mathbf{x}(k-1) + {}^P R_M(k)B(k)\mathbf{x}_M^u(k) + [{}^P R_M(k)B(k)M R_P^o(k) - B(k)]\mathbf{X}^o(k) - {}^P R_M(k)B(k)\Delta^M \mathbf{T}_P(k) + \mathbf{w}(k) \quad (28)$$

By comparing Eq. (28) with Eq. (25), the machined surface deviation  $B(k)\mathbf{x}^u(k)$  at operation  $k$  can be represented as

$$B(k)\mathbf{x}^u(k) = {}^P R_M(k)B(k)\mathbf{x}_M^u(k) + [{}^P R_M(k)B(k)M R_P^o(k) - B(k)]\mathbf{X}^o(k) - {}^P R_M(k)B(k)\Delta^M \mathbf{T}_P(k) \quad (29a)$$

Considering the impacts of datums and fixtures on setup (Eqs. (16) and (21)), we can rewrite Eq. (29a) as

$$B(k)\mathbf{x}^u(k) = {}^P R_F^o(k)F R_M^o(k)B(k)\mathbf{x}_M^u(k) + [{}^P R_F^o(k)\Delta^F R_M(k)B(k)M R_F^o(k)F R_P^o(k)\mathbf{X}^o(k) - {}^P R_F^o(k)F R_M^o(k)B(k)\Delta^F R_M(k)F \mathbf{T}_P^o(k) - {}^P R_F^o(k)F R_M^o(k)B(k)\Delta^M \mathbf{T}_F(k)] + [\Delta^P R_F(k)B(k)F R_P^o(k)\mathbf{X}^o(k) - {}^P R_F^o(k)B(k)\Delta^F \mathbf{T}_P(k)] \quad (29b)$$

*Remark 1* At the right hand side of Eq. (29b), the three terms from left to right are caused by  $\mathbf{e}_k^m$ ,  $\mathbf{e}_k^f$  and  $\mathbf{e}_k^d$  respectively. Since  $\mathbf{e}_k^m$ ,  $\mathbf{e}_k^f$  and  $\mathbf{e}_k^d$  are independent, those three terms are also independent. This suggests that  $B(k)\mathbf{x}^u(k)$  can be separated into three components corresponding to three types of errors.

*Remark 2* Although  $B(k)\mathbf{x}_M^u(k)$  is only affected by the tool path movement,  $B(k)\mathbf{x}^u(k)$  can be contributed by  $\mathbf{e}_k^m$ ,  $\mathbf{e}_k^f$  and  $\mathbf{e}_k^d$ .

*Remark 3* Equations (28) and (29) describe how the error sources affect part accuracy and how the errors propagate in the process.

If we treat part deviation as a state vector, Eq. (25), together with Eqs. (28) and (29), can be thought as a state equation. From Eq. (6), deviation observation for operation  $k$  is written as  $\mathbf{y}(k)$

$= C(k)\mathbf{x}(k) + \mathbf{v}(k)$ . Hence, a state space model is developed to model the dimensional deviation propagation and observation for the machining process.

## 6 Model Validation

A cylinder head is used to validate the proposed modeling methodology. The parts are machined under both normal and faulty conditions. The CMM measurements are compared with model predictions.

Figure 6 shows the part design and specifications. Descriptions of the characteristics are given in Table 1. The association between characteristics and operations is illustrated by the first and the third column in Table 1.

Three operations are performed to meet design specifications (Table 2). Figure 7(a) graphically shows the operational sequence, where  $T_i$ 's ( $i=1,2,\dots,6$ ) are six locators used as datums. The primary datum surface D consists of  $T_1$ ,  $T_2$  and  $T_3$ . Surface M1 represents the cover face M after the first operation on it. The convention applies to other surfaces. Setups, fixtures and locating schemes are shown in Fig. 7(b).

To obtain the repeatability of machine tools and fixtures, an experiment is conducted and the results are as follows: the standard deviation of the angular error component is 0.0001 radians and the standard deviation of the positional error component is 10 microns. The repeatability of size related errors is 20 microns. The fixture repeatability, i.e., the standard deviation of tooling element errors, is 10 microns.

Under normal conditions, the real part was machined and the CMM measurement data is given in Table 5. Then a fault is pur-

Table 2 Operational Sequence and Locating Datums

Operation #	Locating Datums (Primary+Secondary+Tertiary datum)	Operation Descriptions
1	D( $T_1, T_2, T_3$ ) + ( $T_4, T_5$ ) + $T_6$	Mill cover M
2	M1 + ( $T_4, T_5$ ) + $T_6$	Mill joint face A Drill hole B and C
3	A1 + B + C	Mill slot S

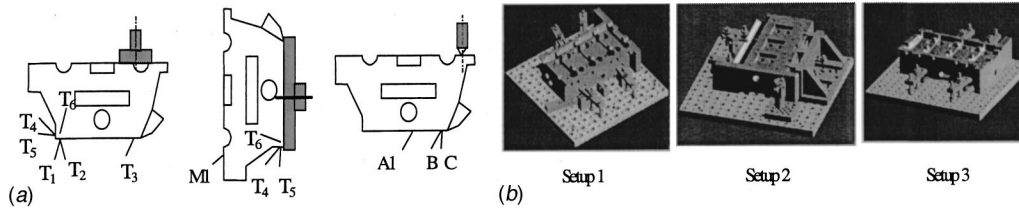


Fig. 7 (a) Operational sequence (b) fixture locating schemes & setups

Table 3 Part Model

$X_i$	$n_x$ (radian)	$n_y$ (radian)	$n_z$ (radian)	$p_x$ (mm)	$p_y$ (mm)	$p_z$ (mm)	$d_1$ (mm)
(1) Surface D	0	0	1	-133.7	134.7	0	0
(2) Joint face A	0	0	1	0	0	-2.5	0
(3) Cover face M	0	0	1	0	0	117.0	0
(4) Hole B	0	0	1	0	0	53.6	15
(5) Hole C	0	0	1	0	306	53.6	15
(6) Slot S	0	0	1	0	0	100.7	0

Table 4 Setup Operations

Entry/unit	F-Coordinate to M-Coordinate (nominal)	P-Coordinate to F-Coordinate (nominal)	Fixture noise	Datum noise	Fixture fault
$\alpha$	0	0	0.0001	0.0001	-0.0020
$\beta$ radian	0	$\pi$	0.0001	0.0001	-0.0025
$\gamma$	0	0	0.0001	0.0001	0.0001
$p_x$	100	0	0.01	0.01	0.01
$p_y$ mm	60	0	0.01	0.01	0.01
$p_z$	80	0	0.01	0.01	0.4

Table 5 Comparison between Measurement and Model Prediction (unit in mm)

Char.#	(1)	(2)	(3)	(4)	(5)	(6)
Spec.	117.0±0.1	2.50±0.1	0.05	15.0±0.05	100.7±0.1	0.05
CMM (normal)	117.096	2.457	0.035	15.034	100.726	0.042
Prediction (normal)	117.048	2.495	0.028	15.000	100.603	0.035
CMM (fault)	117.053	2.320	0.446	15.038	100.816	0.446
Prediction (fault)	117.052	2.349	0.144	15.002	100.931	0.202

posedly introduced into operation 2 by putting a 0.3 mm shim onto a locating pin of the primary datum. Under faulty conditions, the second part was machined with CMM measurement given in Table 5.

The model prediction is performed for comparison study. At first, the part model is built by following the rules given in Section 2. Six surfaces are chosen to model the part (Table 3). The  $xoy$  plane of the P-Coordinate coincides with surface D. Different choices of P-Coordinate make no difference to the outcomes if the choice is consistent during the study. The data in Table 3 is the nominal values for the final operation which are determined by the process planning.

The second step is to model the setup and machining operations. Under normal conditions, only natural variations exist. The fixture noise is generated by assuming that each tooling element follows a normal distribution with zero mean and standard deviation equal to its repeatability. From the process planning, Euler angles of  $\alpha$ ,  $\beta$ , and  $\gamma$  are used to construct rotation matrix  ${}^M R_F^0$

and  ${}^F R_P^0(k)$ , and  $p_x$ ,  $p_y$  and  $p_z$  are for  ${}^M T_F^0$  and  ${}^F T_P^0$ . Under faulty conditions, fixture errors are used to construct matrices  $\Delta {}^M R_F$  and  $\Delta {}^M T_F$  (Described by Eq. (15)).

$\Delta {}^P R_F$  and  $\Delta {}^F T_P$  are caused by datum variations (Described by Eq. (20)). In the first operation, the variability of datum targets  $T_i$ 's ( $i=1,2,\dots,6$ ) is given in Table 4. Random error of datum surface D is generated to take into account workpiece variations. Other datum surfaces used in the remaining operations are the direct output from the machining operations.

The machining simulation is performed based on Eqs. (28) and (29). Developed with Matlab, the program runs in a Pentium III 533 computer with Windows 2000 operation system. 100 parts are run under both normal and faulty conditions. Each run takes less than 20 seconds. By comparing the predicted mean values of characteristics with CMM measurements (Table 5), the discrepancies are small both under normal and faulty conditions. When the 0.3 mm shim is put onto one pin of the primary datum, the discrep-

ancies are relatively larger, e.g., the parallelism between M and A and the parallelism between A and S. As the shim makes the part tilted and increases the cutting depth, the cutting force and fixture stability problems could be the contributing factors that make parallelisms worse. Since those two factors are not modeled, this could be the main reason that explains the discrepancies. However, the model still is able to predict that parallelisms are beyond the tolerance range. As the deviations from tolerance are relatively smaller in real situations, the model predicts well within that area without extreme cutting conditions. Therefore, the discrepancies between model prediction and real measurements are reasonably small.

## 7 Summary

In this paper, a state space model was developed to model the error propagation in MMPs. This is achieved by

- providing a quality-oriented part model: A revised vectorial surface model is applied to facilitate part deviation representation and observation. Only error transmission related surfaces are chosen to build the part model.
- modeling setup, machining operations, and operational sequences: Modeling of setup, machining operations, and operational sequences facilitates deviation propagation analysis. Further, engineering knowledge from process planning can be captured.
- considering errors from datums, fixtures, and machine tools: By using homogenous transformation approach, error transmission is captured by describing the kinematic relationships among three coordinate systems. Fixture errors are modeled in terms of tooling elements and a synthetic machine tool error model is proposed with consideration of both machine tool repeatability and the precision of cutting tool.
- modeling deviation propagation: Part deviations are explicitly separated into three parts, i.e., deviations caused by upstream, fixtures, and machine tools. This separation is extremely important for the causality study and variation analysis.

Since the process variables are directly modeled, tolerance design can be performed without struggling on how to make assumptions about component dimensions. Besides that, design problems such as datum selection, fixture layout design, and process validation can also be studied based on the model. On the other hand, the model provides the basis to monitor the multi-operational process and to determine root causes. Therefore, the proposed model has great potentials in a variety of applications.

## Acknowledgment

The authors gratefully acknowledge the financial support of the NSF Engineering Research Center for Reconfigurable Machining Systems (NSF Grant EEC95-92125) at the University of Michigan and the valuable input from the Center's industrial partners.

## Appendix

**Proposition 1.** The error propagation model in a MMP is proposed as

$$\mathbf{x}(k) = A(k)\mathbf{x}(k-1) + {}^P R_M(k)B(k)\mathbf{x}_M^u(k) + [{}^P R_M(k)B(k)M R_P^o(k) - B(k)]\mathbf{x}^o(k) - {}^P R_M(k)B(k)\Delta^M \mathbf{T}_P(k) + \mathbf{w}(k) \quad (28)$$

*Proof:* For operation  $k$ , the following operations are performed in sequence:

- 1) Setup operation By Eq. (12), setup operation is expressed as

$$\mathbf{X}_M(k-1) = {}^M R_P(k)\mathbf{X}(k-1) + {}^M \mathbf{T}_P(k)$$

- 2) Machining operation By Eq. (23),  $\mathbf{X}_M(k)$  in M-Coordinate turns to be:

$$\mathbf{X}_M(k) = A(k)\mathbf{X}_M(k-1) + B(k)\mathbf{X}_M^u(k)$$

- 3) Unload part from machine tool Part  $\mathbf{X}(k)$  in P-Coordinate is

$$\begin{aligned} \mathbf{X}(k) &= {}^P R_M(k)[\mathbf{X}_M(k) - {}^M \mathbf{T}_P(k)] \\ &= {}^P R_M(k)\{A(k)[{}^M R_P(k)\mathbf{X}(k-1) \\ &\quad + {}^M \mathbf{T}_P(k)] + B(k)\mathbf{X}_M^u(k)\} - {}^P R_M(k)M \mathbf{T}_P(k) \\ &= {}^P R_M(k)A(k)M R_P(k)\mathbf{X}(k-1) + {}^P R_M(k)B(k)\mathbf{X}_M^u(k) \\ &\quad + {}^P R_M(k)(k)A(k)M \mathbf{T}_P(k) \\ &\quad - {}^P R_M(k)[A(k) + B(k)]M \mathbf{T}_P(k) \\ &= {}^P R_M(k)A(k)M R_P(k)\mathbf{X}(k-1) \\ &\quad + {}^P R_M(k)B(k)[\mathbf{X}_M^u(k) - {}^M \mathbf{T}_P(k)] \end{aligned}$$

As  ${}^P R_M(k)M R_P(k) = I$ , we have  ${}^P R_M(k)A(k)M R_P(k) = A(k)$ .  $\mathbf{X}(k)$  turns to be

$$\mathbf{X}(k) = A(k)\mathbf{X}(k-1) + {}^P R_M(k)B(k)[\mathbf{X}_M^u(k) - {}^M \mathbf{T}_P(k)]$$

The part deviation after operation  $k$  is  $\mathbf{x}(k) = \mathbf{X}(k) - \mathbf{X}^o(k)$ . It is further expressed as

$$\begin{aligned} \mathbf{x}(k) &= A(k)\mathbf{X}(k-1) + {}^P R_M(k)B(k)[\mathbf{X}_M^u(k) - {}^M \mathbf{T}_P(k)] - \mathbf{X}^o(k) \\ &= A(k)\mathbf{X}(k-1) + {}^P R_M(k)B(k)[\mathbf{X}_M^u(k) - \mathbf{X}_M^o(k) + \mathbf{X}_M^o(k) \\ &\quad - {}^M \mathbf{T}_P(k)] - [A(k) + B(k)]\mathbf{X}^o(k) \end{aligned}$$

As operation  $k$  does not change  $A(k)\mathbf{X}(k-1)$ ,  $A(k)\mathbf{X}^o(k) = A(k)\mathbf{X}^o(k-1)$  holds. Then

$$\begin{aligned} \mathbf{x}(k) &= A(k)\mathbf{x}(k-1) + {}^P R_M(k)B(k)[\mathbf{X}_M^u(k) - \mathbf{X}_M^o(k)] \\ &\quad + {}^P R_M(k)B(k)\mathbf{X}_M^o(k) - {}^P R_M(k)B(k)M \mathbf{T}_P(k) - B(k)\mathbf{X}^o(k) \end{aligned}$$

As  $\mathbf{X}_M^o(k) = {}^M R_P^o(k)\mathbf{X}^o(k) + {}^M \mathbf{T}_P^o(k)$  and  $\mathbf{x}_M^u(k) = \mathbf{X}_M^u(k) - \mathbf{X}_M^o(k)$ ,  $\mathbf{x}(k)$  can be rewritten as

$$\begin{aligned} \mathbf{x}(k) &= A(k)\mathbf{x}(k-1) + {}^P R_M(k)B(k)\mathbf{x}_M^u(k) \\ &\quad + {}^P R_M(k)B(k)[{}^M R_P^o(k)\mathbf{X}^o(k) + {}^M \mathbf{T}_P^o(k)] \\ &\quad - {}^P R_M(k)B(k)M \mathbf{T}_P(k) - B(k)\mathbf{X}^o(k) \\ &= A(k)\mathbf{x}(k-1) + {}^P R_M(k)B(k)\mathbf{x}_M^u(k) \\ &\quad + [{}^P R_M(k)B(k)M R_P^o(k) - B(k)]\mathbf{X}^o(k) \\ &\quad - {}^P R_M(k)B(k)[{}^M \mathbf{T}_P(k) - {}^M \mathbf{T}_P^o(k)] + \mathbf{w}(k) \end{aligned}$$

Then we have Eq. (28).  $\mathbf{w}(k)$  is added process noise term.

## Nomenclature

- $\mathbf{e}_k^f$  = fixture error at operation  $k$
- $\mathbf{e}_k^d$  = datum error at operation  $k$
- $\mathbf{e}_k^m$  = machine tool error at operation  $k$
- $\mathbf{w}(k) \& \mathbf{v}(k)$  = noise terms in the state space equation for operation  $k$
- $\mathbf{X}$  = a vector used to describe a part
- $\mathbf{X}(k)$  = part machined after operation  $k$ , represented in the  $P$  (part) coordinate
- $\mathbf{Y}(k)$  = part measurement at operation  $k$
- $\mathbf{x}(k)$  = deviation of  $\mathbf{X}(k)$ , represented in the  $P$  coordinate
- $\mathbf{x}_M$ , or  $\mathbf{x}_F$  = deviation of  $\mathbf{X}$ , represented in the  $M$  (Machine) coordinate or the  $F$  (Fixture) coordinate
- $\mathbf{y}(k)$  = deviation of  $\mathbf{Y}(k)$
- $B(k)$  = indicator matrix which labels all surfaces that are machined at operation  $k$
- $A(k)$  = defined as  $A(k) = I - B(k)$ , indicating surfaces not machined at operation  $k$
- $C(k)$  = sensitivity matrix that relates  $\mathbf{x}(k)$  to  $\mathbf{y}(k)$

- $D(k)$  = datum selection matrix used to label the datum surfaces for operation  $k$
- $B(k)\mathbf{x}^u(k)$  = machined surface deviation at operation  $k$
- $Z^o$  = nominal value of variable  $Z$
- ${}^iR_j(k)$  = rotation transformation from the  $j$  coordinate to the  $i$  coordinate at operation  $k, i, j = P, F, M$
- ${}^iT_j(k)$  = translation transformation from the  $j$  coordinate to the  $i$  coordinate at operation  $k, i, j = P, F, M$

## References

- [1] Fortini, E. T., 1967, *Dimensioning for Interchangeable Manufacture*, Industrial Press, NY.
- [2] Gilson, J., 1951, *A New Approach to Engineering Tolerances*, The Machinery Publishing Co., London, UK.
- [3] Greenwood, W. H., and Chase, K. W., 1987, "A New Tolerance Analysis Method for Designers and Manufactures," *ASME J. Ind.*, **109**, pp. 112–116.
- [4] Ding, Y., Jin, J., Ceglarek, D., and Shi, J., 2002, "Process-Oriented Tolerancing for Multi-Station Assembly System," *IIE Transactions on Design and Manufacturing* (to appear).
- [5] Jin, J., and Shi, J., 1999, "State Space Modeling of Sheet Metal Assembly for Dimensional Control," *ASME J. Manuf. Sci. Eng.*, **121**, pp. 756–762.
- [6] Ding, Y., Shi, J., and Ceglarek, D., 2002, "Diagnosability Analysis of Multi-Station Manufacturing Processes," *ASME Transactions, Journal of Dynamics Systems, Measurement, and Control*, Vol. 124, pp. 1–13.
- [7] Mantripragada, R., and Whitney, D. E., 1999, "Modeling and Controlling Variation Propagation in Mechanical Assemblies Using State Transition Models," *IEEE Robotics and Automation*, **15**, pp. 124–140.
- [8] Lawless, J. F., Mackay, R. J., and Robinson, J. A., 1999, "Analysis of Variation Transmission in Manufacturing Processes—Part I," *J. Quality Technol.*, **31**, pp. 131–142.
- [9] Agrawal, R., Lawless, J. F., and Mackay, R. J., 1999, "Analysis of Variation Transmission in Manufacturing Processes—Part II," *J. Quality Technol.*, **31**, pp. 143–154.
- [10] Cai, W., Hu, S. J., and Yuan, J. X., 1997, "Variational Method of Robust Fixture Configuration Design for 3-D Workpiece," *ASME J. Manuf. Sci. Eng.*, **119**, pp. 593–602.
- [11] Choudhuri, S. A., and De Meter, E. C., 1999, "Tolerance Analysis of Machining Fixture Locators," *ASME J. Manuf. Sci. Eng.*, **121**, pp. 273–281.
- [12] Chen, J. S., Yuan, J. X., Ni, J., and Wu, S. M., 1993, "Real-time Compensation for Time-variant Volumetric Errors on a Machining Center," *ASME J. Ind.*, **115**, pp. 472–479.
- [13] Martinsen, K., 1993, "Vectorial Tolerancing for All Types of Surfaces," *ASME Advances in Design Automation*, Vol. 2, pp. 187–198.
- [14] ASME, *Y14.5 M Dimensioning and Tolerancing*, 1994.
- [15] Frey, D. D., Otto, K. N., and Pflager, W., 1997, "Swept Envelopes of Cutting Tools in Integrated Machine and Workpiece Error Budgeting," *CIRP Ann.*, **46**, pp. 475–480.